

# Unimodular Diffusion and Interacting Vacuum Cosmology

Gopal Kashyap<sup>1\*</sup> and Naveen K. Singh<sup>2†</sup>

<sup>1</sup>Department of Physics, School of Advanced Sciences,

Vellore Institute of Technology, Vellore 632014, Tamil Nadu, India

<sup>2</sup>Sir P. T. Sarvajani College of Science (Autonomous),

Surat 395001, Gujarat, India

## Abstract

We investigate the correspondence between unimodular diffusion cosmology and interacting dark sector models at the background and linear perturbation levels. In the diffusion framework, the effective cosmological constant becomes time-dependent,  $\Lambda(t)$ , sourced by a diffusion current. We show that at background level this framework can be mapped onto interacting dark energy models with  $w = -1$  and energy transfer  $Q$ . Using two common parameterizations,  $Q = \xi H \rho_{de}$  and  $Q = \xi H \rho_{dm}$ , and data from supernovae, DESI BAO, cosmic chronometers, and CMB distance priors, we find  $\xi = -0.0197 \pm 0.0076$  for the vacuum-coupled case, while the matter-coupled case gives a best-fit  $\xi = 0.0018$  with comparable fit. At linear perturbations, the diffusion framework is perturbatively equivalent only to interacting vacuum models with homogeneous energy transfer ( $Q \propto \rho_{de}$ ,  $\delta Q = 0$ ). Including redshift-space distortion data, we obtain  $\xi = -0.0147 \pm 0.0075$ , consistent with  $\Lambda$ CDM ( $\xi = 0$ ) at  $2\sigma$ . The inferred clustering amplitude is  $S_8 = 0.782 \pm 0.026$  for the diffusion model, compared to  $S_8 = 0.77 \pm 0.025$  for  $\Lambda$ CDM under the same dataset, showing a modest impact on structure growth.

## 1 Introduction

Cosmological observations indicate that the present Universe is undergoing an accelerated expansion driven by components whose physical origin remains unknown. Within the framework of modern cosmology, a wide range of phenomena, including cosmic inflation, the cosmic microwave background (CMB), large-scale structure formation, and late-time acceleration, are successfully described by the  $\Lambda$ CDM model. In this model the total energy budget of the Universe consists primarily of dark energy, dark matter, baryonic matter, and radiation. Current observations suggest that dark energy contributes approximately  $\Omega_{de} \simeq 0.68$ , dark matter  $\Omega_{dm} \simeq 0.27$ , and baryons  $\Omega_b \simeq 0.049$  to the total energy density of the Universe [1]. The equation-of-state parameter of dark energy inferred from Planck observations is consistent with a cosmological constant,  $\omega_\Lambda = -1.03 \pm 0.03$  [1].

The  $\Lambda$ CDM model has been remarkably successful at explaining a wide range of cosmological observations, yet it still struggles with some conceptual and observational puzzles. These include the cosmological constant problem, the coincidence problem, and potential tensions between different cosmological datasets. For example, measurements of the Hubble constant  $H_0$  inferred from CMB observations differ from those obtained from local distance ladder measurements such as those from the SH0ES collaboration [2] and strong-lensing observations by the H0LiCOW collaboration [3]. In addition, recent analyses of DESI data suggest a mild preference for an equation-of-state parameter slightly different from  $w = -1$  [4, 5]. These issues

---

\*Email: gplkumar87@gmail.com

†Email: naveen.nkumars@gmail.com

motivate the exploration of alternative models of dark energy and modifications of the standard cosmological framework [6–15].

Among the many attempts to go beyond  $\Lambda$ CDM, interacting dark energy has emerged as one such model. In such models the dark matter and dark energy components are allowed to exchange energy, leading to modified conservation equations for the individual components while preserving the conservation of the total energy–momentum tensor. Interacting dark energy models have been explored as possible mechanisms for alleviating the Hubble tension and the  $S_8$  tension, as well as addressing the coincidence problem [16–20]. Since the microscopic nature of the dark sector is unknown, a variety of phenomenological interaction terms have been proposed in the literature, typically characterized by a coupling function  $Q$  describing the rate of energy transfer between dark matter and dark energy. Commonly studied examples include interactions proportional to the dark matter density or the dark energy density.

Recent studies have also explored interacting dark sector models in the context of the latest cosmological observations, including DESI measurements [21–23]. For instance, in Ref. [16] the interaction term is taken to be proportional to the dark matter energy density, while in Ref. [24] the decay of dark matter into dark radiation has been discussed as a possible mechanism to address both the Hubble tension and the  $S_8$  tension.

In this work we investigate a related framework based on diffusion in the context of unimodular gravity. Diffusion processes in unimodular cosmology have been studied in several works [25–27]. In these models an effective energy transfer occurs between dark matter and a dynamical vacuum component, arising from small violations of energy-momentum conservation that can naturally appear in unimodular gravity [28].

Although diffusion models share certain phenomenological similarities with interacting dark energy models, the physical origin of the energy exchange is fundamentally different. In conventional interacting dark energy models the total energy-momentum tensor of the dark sector remains conserved, while individual components exchange energy through a phenomenological interaction term. In contrast, within the diffusion framework, the apparent non-conservation emerges from the structure of the gravitational theory itself rather than from an explicit coupling introduced in the matter sector.

In unimodular gravity theory the determinant of the metric is fixed, effectively removing the trace part of Einstein’s field equations. As a consequence, the cosmological constant does not appear as a fundamental parameter in the action but instead arises as an integration constant of the field equations. Various aspects and extensions of unimodular gravity have been extensively explored in the literature (see, e.g., Refs. [29–47]).

In unimodular gravity the trace-free Einstein equations can be written as

$$R_{\mu\nu} - \frac{1}{4}g_{\mu\nu}R = 8\pi G \left( T_{\mu\nu} - \frac{1}{4}g_{\mu\nu}T \right). \quad (1)$$

Taking the covariant divergence of the corresponding field equations leads to a modified conservation relation,

$$8\pi G \nabla_\mu T^\mu_\nu = \frac{1}{4} \nabla_\nu (R + 8\pi GT). \quad (2)$$

This relation allows for an effective energy exchange term that can be interpreted as a diffusion process in the dark sector.

Introducing an effective diffusion function  $P(t)$ , the modified conservation equation for dark matter can be written as

$$\dot{\rho}_{\text{dm}} + 3H(\rho_{\text{dm}} + p_{\text{dm}}) = -\dot{P}. \quad (3)$$

Identifying  $Q = \dot{P}$ , the diffusion model can be formally compared with interacting dark energy models characterized by phenomenological interaction terms such as  $Q = \xi H \rho_{\text{dm}}$  or  $Q = \xi H \rho_{\text{de}}$ . This correspondence provides a useful framework for studying the cosmological implications of diffusion within the well-developed phenomenology of interacting dark sector models.

The main goal of this paper is to investigate the relationship between unimodular diffusion and interacting dark energy models and to examine whether these models can be distinguished observationally. In particular, we study the background evolution and the growth of cosmological perturbations, and confront the model predictions with current observational data. We use recent cosmological observations including the Pantheon+ SNIa compilation, measurements of the Hubble parameter  $H(z)$ , baryon acoustic oscillation data, redshift-space distortion (RSD) measurements, and CMB distance priors to constrain the model parameters.

The paper is organized as follows. Section 2 reviews interacting dark sector models. Section 3 presents the diffusion dynamics and its mapping onto interacting dark sector models. The background cosmological equations are introduced in Section 4. The datasets and methodology used in our analysis are described in Section 5. Section 6 presents the observational constraints and model comparison. Linear perturbations and the growth of structure are discussed in Section 7. Finally, our conclusions are summarized in Section 8.

## 2 Review of Interacting Dark Sector Models

Interacting dark sector models allow for an exchange of energy between dark matter and dark energy through a phenomenological interaction term  $Q$ . In such case the individual components are not conserved separately, although the total energy-momentum tensor remains conserved.

Assuming pressureless dark matter ( $p_{dm} = 0$ ) and dark energy with equation of state

$$p_{de} = \omega_{de}\rho_{de}, \quad (4)$$

the continuity equations for the dark sector components can be written as

$$\dot{\rho}_{dm} + 3H\rho_{dm} = -Q, \quad (5)$$

$$\dot{\rho}_{de} + 3H(1 + \omega_{de})\rho_{de} = Q. \quad (6)$$

With this convention,  $Q > 0$  corresponds to energy transfer from dark matter to dark energy, while  $Q < 0$  represents the reverse process. Since the microscopic origin of the dark sector interaction is unknown, the functional form of  $Q$  is typically introduced phenomenologically. Two commonly studied interaction forms are

$$Q = \xi H \rho_{dm}, \quad Q = \xi H \rho_{de}, \quad (7)$$

where  $\xi$  is a dimensionless coupling parameter.

For the interaction  $Q = \xi H \rho_{dm}$ , Eq. (5) can be solved analytically, yielding

$$\rho_{dm}(a) = \rho_{dm0} a^{-3-\xi}. \quad (8)$$

Thus the interaction modifies the standard dilution law of matter. For  $\xi = 0$  the standard  $\Lambda$ CDM scaling  $\rho_{dm} \propto a^{-3}$  is recovered, while negative (positive) values of  $\xi$  lead to a slower (faster) dilution of dark matter.

We now consider the interaction  $Q = \xi H \rho_{de}$ . For illustration we adopt a time-dependent equation-of-state parameter of the form

$$\omega_{de}(a) = -1 + \alpha a + \beta a^2, \quad (9)$$

which allows small deviations from a cosmological constant.

Using Eq. (6) and transforming derivatives to the scale factor via  $d/dt = aH d/da$ , the dark energy density evolves as

$$\rho_{de}(a) = \rho_{de0} a^\xi \exp \left[ -3 \left( \alpha(a-1) + \frac{\beta}{2}(a^2-1) \right) \right]. \quad (10)$$

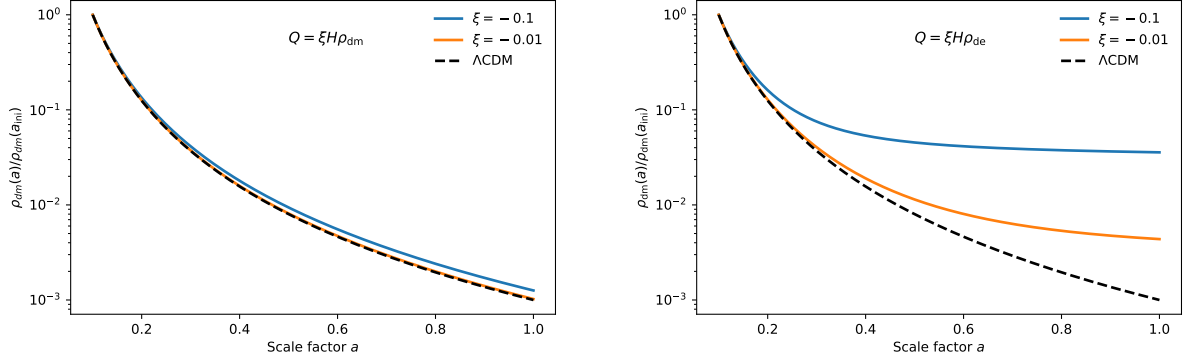


Figure 1: Evolution of the normalized dark matter density for interacting dark sector models. *Left*: interaction  $Q = \xi H \rho_{dm}$  showing the modified dilution law  $\rho_{dm} \propto a^{-3-\xi}$ . *Right*: interaction  $Q = \xi H \rho_{de}$  where the matter density evolution depends on the dark energy dynamics.

Substituting this result into Eq. (5), the dark matter density satisfies

$$\frac{d\rho_{dm}}{da} + \frac{3}{a}\rho_{dm} = -\xi \rho_{de0} a^{\xi-1} \exp\left[-3\left(\alpha(a-1) + \frac{\beta}{2}(a^2-1)\right)\right]. \quad (11)$$

Solving this first-order equation gives

$$\rho_{dm}(a) = a^{-3} \left[ \rho_{dm0} - \xi \rho_{de0} \int_1^a a'^{\xi+2} \exp\left[-3\left(\alpha(a'-1) + \frac{\beta}{2}(a'^2-1)\right)\right] da' \right]. \quad (12)$$

This expression shows explicitly that the dark matter density receives a contribution sourced by the evolving dark energy component.

The different interaction prescriptions lead to distinct modifications of the matter density evolution. For the coupling  $Q = \xi H \rho_{dm}$  the matter density follows a simple power-law scaling  $a^{-3-\xi}$ , whereas for  $Q = \xi H \rho_{de}$  the evolution depends on the dark energy dynamics through the above integral solution. The resulting behavior of  $\rho_{dm}(a)$  for the considered interaction models is shown in Fig. 1. For the numerical analysis we choose  $\alpha = 0.01$  and  $\beta = 0.001$ , which correspond to small departures from the  $\Lambda$ CDM limit ( $w = -1$ ) and therefore serve only to demonstrate the qualitative effect of the interaction on the matter density evolution. The evolution of the normalized dark matter density for the case ( $Q = \xi H \rho_{dm}$ ) deviates relatively little from the standard  $\Lambda$ CDM behavior, and the matter density evolves close to the usual  $a^{-3}$  scaling. In contrast, for ( $Q = \xi H \rho_{de}$ ), the interaction significantly modifies the dilution rate of dark matter, leading to a noticeably slower decrease of  $\rho_{dm}$  for negative values of  $\xi$ . The effect becomes stronger as  $\xi$  increases, illustrating how the interaction parameter controls the energy transfer in the dark sector.

These interacting dark sector models provide a useful phenomenological framework for describing energy exchange in the dark sector. In the next section we show that the diffusion model arising from unimodular gravity can be mapped onto a specific class of interacting vacuum models, leading to an exact degeneracy at the background level.

### 3 Diffusion dynamics and mapping to interacting running vacuum models

In unimodular gravity the conservation of the energy-momentum tensor is modified by the presence of a diffusion current. The generalized conservation equation takes the form

$$\nabla_{\mu} T^{\mu\nu} = J^{\nu}, \quad (13)$$

where  $J^\nu$  describes the diffusion of energy between matter and the vacuum sector. For a homogeneous and isotropic FLRW universe the time component of this equation leads to a modified continuity equation for dark matter,

$$\dot{\rho}_{\text{dm}} + 3H\rho_{\text{dm}} = -\dot{P}, \quad (14)$$

where  $P(t)$  denotes the diffusion function.

In unimodular gravity the Lagrange multiplier  $\lambda$  appearing in the field equations behaves as a dynamical vacuum contribution. Its evolution is related to the diffusion process through

$$\dot{\lambda} = 8\pi G \dot{P}. \quad (15)$$

It is therefore convenient to define an effective vacuum energy density

$$\rho_{\text{de}} \equiv \frac{\lambda}{8\pi G}. \quad (16)$$

Using this definition we obtain

$$\dot{\rho}_{\text{de}} = \dot{P}. \quad (17)$$

Eqs. (14) and (17) can be written in the same form as the continuity equations of interacting dark sector models,

$$\dot{\rho}_{\text{dm}} + 3H\rho_{\text{dm}} = -Q, \quad (18)$$

$$\dot{\rho}_{\text{de}} + 3H(1 + w_{\text{de}})\rho_{\text{de}} = Q, \quad (19)$$

by identifying the interaction term

$$Q = \dot{P}. \quad (20)$$

Comparison with Eq. (17) shows that consistency requires

$$w_{\text{de}} = -1, \quad (21)$$

indicating that the effective dark energy component behaves as a vacuum energy with equation of state  $w = -1$ .

The relation  $Q = \dot{P}$  therefore establishes a direct connection between the diffusion process and interacting dark sector models. However, the diffusion framework does not uniquely determine the functional dependence of the interaction term on the dark sector densities. In phenomenological studies it is common to parameterize the interaction rate as proportional to the Hubble expansion rate and one of the dark sector densities. Following the discussion in Sec. 2, we therefore consider the two widely studied interaction models

$$Q = \xi H \rho_{\text{de}}, \quad Q = \xi H \rho_{\text{dm}}, \quad (22)$$

where  $\xi$  is a dimensionless coupling parameter.

These parameterizations can be interpreted as different phenomenological aspects of the diffusion source term  $Q = \dot{P}$ . Consequently, once the interaction term is specified, the unimodular diffusion model can be mapped onto interacting dark sector models at the level of the homogeneous background evolution. The resulting cosmological expansion histories are therefore degenerate and cannot be distinguished using background observables alone.

This degeneracy can be broken at the level of cosmological perturbations. While the background dynamics depend only on the effective interaction term  $Q$ , the perturbation equations retain sensitivity to the physical origin of the interaction. As a result, diffusion-driven vacuum dynamics can in principle be distinguished from phenomenological interacting vacuum models through large-scale structure, anisotropy, and growth-rate observations.

## 4 Background Dynamics and Observables

We consider a spatially flat Friedmann-Lemaître-Robertson–Walker (FLRW) universe composed of radiation ( $r$ ), baryons ( $b$ ), dark matter (dm), and dark energy (de). Radiation and baryons are assumed to be separately conserved, while an interaction is allowed between dark matter and dark energy. The corresponding continuity equations are

$$\dot{\rho}_r + 4H\rho_r = 0, \quad (23)$$

$$\dot{\rho}_b + 3H\rho_b = 0, \quad (24)$$

$$\dot{\rho}_{\text{dm}} + 3H\rho_{\text{dm}} = -Q, \quad (25)$$

$$\dot{\rho}_{\text{de}} + 3H(1 + w_{\text{de}})\rho_{\text{de}} = Q, \quad (26)$$

where  $Q$  denotes the energy transfer between the dark sector components. Following the mapping discussed in Sec. 3, we impose  $w_{\text{de}} = -1$  and identify the interaction parameter of the interacting dark sector model with the diffusion coupling parameter.

The Friedmann equations retain their standard form,

$$H^2 = \frac{8\pi G}{3}(\rho_r + \rho_b + \rho_{\text{dm}} + \rho_{\text{de}}), \quad (27)$$

$$\dot{H} = -4\pi G(\rho_r + \rho_b + \rho_{\text{dm}} + \rho_{\text{de}} + P_{\text{de}} + P_r). \quad (28)$$

For vacuum-like dark energy ( $w_{\text{de}} = -1$ ), the dark energy pressure satisfies  $P_{\text{de}} = -\rho_{\text{de}}$ . Substituting this relation into the Raychaudhuri equation gives

$$\dot{H} = -4\pi G\left(\rho_{\text{dm}} + \rho_b + \frac{4}{3}\rho_r\right). \quad (29)$$

Although the interaction term  $Q$  does not appear explicitly in Eq. (29), its effects are encoded in the evolution of the dark matter and dark energy densities through the modified continuity equations.

### 4.1 Deceleration parameter and effective equation of state

The deceleration parameter is defined as

$$q \equiv -1 - \frac{\dot{H}}{H^2}. \quad (30)$$

Using the Friedmann and Raychaudhuri equations, Eqs. (27) and (29), this can be expressed in terms of the total energy density and pressure as

$$q = \frac{1}{2}\left(1 + 3\frac{p_{\text{tot}}}{\rho_{\text{tot}}}\right) = \frac{1}{2}(1 + 3w_{\text{eff}}), \quad (31)$$

where we define the effective equation of state

$$w_{\text{eff}} \equiv \frac{p_{\text{tot}}}{\rho_{\text{tot}}}. \quad (32)$$

For a universe containing radiation, baryons, dark matter, and vacuum energy with  $w_{\text{de}} = -1$ , the deceleration parameter can be written as

$$q = -1 + \frac{3}{2}\frac{\rho_{\text{dm}} + \rho_b + \frac{4}{3}\rho_r}{\rho_r + \rho_b + \rho_{\text{dm}} + \rho_{\text{de}}}. \quad (33)$$

Equivalently, in terms of the density parameters,

$$q = -1 + \frac{3}{2} \left( \Omega_{\text{dm}} + \Omega_b + \frac{4}{3} \Omega_r \right). \quad (34)$$

The functional forms of Eqs. (31) and (33) follow directly from the background field equations and are therefore independent of the explicit form of the dark sector interaction. However, different interaction terms modify the redshift evolution of the individual energy densities, leading to distinct histories for  $w_{\text{eff}}(z)$  and  $q(z)$ .

## 5 Data and Methodology

We now test the interacting dark sector models against cosmological data. As shown in Sec. 3, these models have the same background expansion history as unimodular diffusion, making them observationally equivalent at the background level.

### 5.1 Datasets

The analysis incorporates the following observational datasets:

- **Cosmic chronometers:** We use 32 measurements of the Hubble expansion rate obtained from the cosmic chronometer (CC) method. See Table 1 and the references. This approach estimates  $H(z)$  directly from the differential age evolution of the galaxies, using the relation  $H(z) = -\frac{1}{1+z} \frac{dz}{dt}$  [48]. Since it relies only on the relative ages of galaxies, the CC technique provides a model independent probe of the expansion history without assuming a specific cosmological model.
- **Type Ia Supernovae (Pantheon+):** We use the Pantheon+ compilation of Type Ia Supernovae (SNIa)<sup>1</sup> [49], which contains 1701 light curve measurements corresponding to 1550 unique spectroscopically confirmed SNIa spanning the redshift range  $0.001 < z < 2.26$ . The additional light curves arise from repeated observations of certain objects, including supernova siblings, multiple supernovae occurring in the same host galaxy, as well as SNIa located in Cepheid calibrated host galaxies that are used to anchor the distance scale.
- **Baryon Acoustic Oscillations (DESI DR2):** We further include baryon acoustic oscillation (BAO) measurements from the second data release of the Dark Energy Spectroscopic Instrument (DESI DR2)<sup>2</sup> [50]. BAO observations provide a standard ruler set by the sound horizon at the baryon drag epoch and probe the expansion history through measurements of the comoving angular diameter distance and the Hubble parameter at different redshifts.
- **CMB distance priors:** For the cosmic microwave background (CMB) we use distance priors derived from the *Planck* 2018 observations [51]. This approach efficiently constrains background cosmology while avoiding a full Boltzmann analysis.

---

<sup>1</sup>[https://github.com/CobayaSampler/sn\\_data](https://github.com/CobayaSampler/sn_data)

<sup>2</sup>[https://github.com/CobayaSampler/bao\\_data/tree/master/desi\\_bao\\_dr2](https://github.com/CobayaSampler/bao_data/tree/master/desi_bao_dr2)

Table 1: The 32 observational data points of  $H(z)$  with  $1\sigma$  uncertainties used in present work.

$z$	$H(z)$	$\sigma_H$	Ref.	$z$	$H(z)$	$\sigma_H$	Ref.
0.07	69.0	19.6	[52]	0.4783	83.8	10.2	[53]
0.09	69	12	[54]	0.48	97.0	62.0	[55]
0.12	68.6	26.2	[52]	0.5929	107.0	15.5	[56]
0.17	83.0	8.0	[57]	0.6797	95.0	10.5	[56]
0.1791	78.0	6.2	[56]	0.75	98.8	33.6	[58]
0.1993	78.0	6.9	[56]	0.7812	96.5	12.5	[56]
0.20	72.9	29.6	[52]	0.8754	124.5	17.4	[56]
0.27	77.0	14.0	[57]	0.88	90.0	40.0	[55]
0.28	88.8	36.6	[52]	0.9	117	23	[57]
0.3519	85.5	15.7	[56]	1.037	133.5	17.6	[56]
0.3802	83	13.5	[53]	1.3	168.0	17.0	[57]
0.4	95	17	[57]	1.363	160.0	33.8	[59]
0.4004	79.9	11.4	[53]	1.43	177.0	18.0	[57]
0.4247	90.4	12.8	[53]	1.53	140.0	14.0	[57]
0.4497	96.3	14.4	[53]	1.75	202.0	40.0	[57]
0.47	89.0	49.6	[60]	1.965	186.5	50.6	[59]

## 5.2 Corrected supernova magnitude

To avoid assuming light curve corrections calibrated within a  $\Lambda$ CDM framework, we fit the supernova nuisance parameters  $(\alpha, \beta, \gamma, M_0)$  simultaneously with the cosmological parameters, following [61].

For each Type Ia supernova the standardized apparent magnitude is constructed using the SALT2 light-curve parameters,

$$m_{B,i}^{\text{corr}} = m_{B,i} + \alpha x_{1,i} - \beta c_i + \gamma G_{\text{host},i}, \quad (35)$$

where  $m_{B,i}$  is the observed peak magnitude,  $x_{1,i}$  and  $c_i$  are the stretch and color parameters, and  $G_{\text{host},i}$  accounts for the host-galaxy mass step,

$$G_{\text{host},i} = \begin{cases} +0.5, & \log_{10}(M_{\text{host}}/M_{\odot}) \geq 10, \\ -0.5, & \log_{10}(M_{\text{host}}/M_{\odot}) < 10. \end{cases} \quad (36)$$

For Hubble-flow supernovae, the theoretical distance modulus is

$$\mu_{\text{th}}(z, \theta) = 5 \log_{10} \left[ \frac{d_L(z, \theta)}{\text{Mpc}} \right] + 25, \quad (37)$$

where  $d_L(z, \theta)$  is the luminosity distance for cosmological parameters  $\theta$ . The residual vector is

$$\Delta\mu_i^{\text{SN}} = m_{B,i}^{\text{corr}} - M_0 - \mu_{\text{th}}(z_i, \theta), \quad (38)$$

with corresponding  $\chi^2$

$$\chi_{\text{HF}}^2 = (\Delta\mu^{\text{SN}})^T \mathbf{C}_{\text{SN}}^{-1} \Delta\mu^{\text{SN}}, \quad (39)$$

where  $\mathbf{C}_{\text{SN}}$  is the Pantheon+ covariance matrix restricted to the Hubble-flow sample.

For Cepheid-host calibrator supernovae, the distance modulus is taken from the SHOES distance ladder,

$$\Delta\mu_i^{\text{Cph}} = m_{B,i}^{\text{corr}} - M_0 - \mu_i^{\text{SHOES}}, \quad (40)$$

with  $\chi^2$

$$\chi_{\text{Cph}}^2 = (\Delta\mu^{\text{Cph}})^T \mathbf{C}_{\text{Cph}}^{-1} \Delta\mu^{\text{Cph}}. \quad (41)$$

### 5.3 Total likelihood and parameter estimation

The total supernova contribution is given by

$$\chi_{\text{SN}}^2 = \chi_{\text{HF}}^2 + \chi_{\text{Cph}}^2, \quad (42)$$

The full parameter vector sampled in the analysis is

$$\Theta = \{\theta_{\text{cosmo}}, \alpha, \beta, \gamma, M_0\}, \quad (43)$$

where  $\theta_{\text{cosmo}}$  denotes the cosmological parameters and  $(\alpha, \beta, \gamma, M_0)$  are the supernova nuisance parameters.

Joint constraints are obtained by combining all datasets,

$$\chi_{\text{tot}}^2 = \chi_{H(z)}^2 + \chi_{\text{SN}}^2 + \chi_{\text{BAO}}^2 + \chi_{\text{CMB}}^2, \quad (44)$$

corresponding to the likelihood

$$\mathcal{L}_{\text{tot}} = \mathcal{L}_{H(z)} \mathcal{L}_{\text{SN}} \mathcal{L}_{\text{BAO}} \mathcal{L}_{\text{CMB}}. \quad (45)$$

For the interacting models considered here, the primary cosmological parameter set is

$$\{H_0, \Omega_{b0}, \Omega_{\text{dm}0}, \xi\}, \quad (46)$$

The radiation density parameter is fixed to its standard value. We explore the posterior distribution of the model parameters using the `emcee` Python package, an implementation of the affine invariant ensemble sampler for Markov Chain Monte Carlo methods [62].

## 6 Background constraints and model comparison

In Fig. 2, we present the marginalized one and two dimensional posterior distributions of the cosmological parameters  $\{H_0, \Omega_{m0}, \Omega_{b0}, \xi\}$  obtained from a joint analysis of  $H(z)$ , BAO DESI DR2, Pantheon+ SNIa, and CMB distance priors. The red contours correspond to the vacuum proportional interaction  $Q = \xi H \rho_{\text{de}}$ , while the blue contours represent the matter-proportional interaction  $Q = \xi H \rho_{\text{dm}}$ . For comparison, we also considered the standard  $\Lambda$ CDM model and the constant equation of state  $w$ CDM model. A quantitative summary of the parameter constraints and model comparison statistics is presented in Table 2.

The standard cosmological parameters  $H_0$ ,  $\Omega_{m0}$ , and  $\Omega_{b0}$  are tightly constrained and show substantial overlap between the two interaction models. This demonstrates that background cosmological data robustly determine the global expansion parameters largely independently of the detailed modeling of the dark sector. In particular, the inferred values of  $H_0$  cluster around  $H_0 \simeq 68 \text{ km s}^{-1} \text{ Mpc}^{-1}$  for all models considered, with no significant shifts induced by the inclusion of an interaction or a free dark energy equation of state.

In comparison, the effective coupling parameter  $\xi$  shows a clear dependence on the assumed interaction prescription. For the matter-proportional interaction  $Q = \xi H \rho_{\text{dm}}$ , we obtain  $\xi = 0.0018 \pm 0.0031$ , which is tightly consistent with zero and indicates that background observations strongly suppress deviations from standard dark matter conservation. For the vacuum-proportional interaction  $Q = \xi H \rho_{\text{de}}$ , the posterior distribution is broader, giving  $\xi = -0.0197 \pm 0.0076$ , with a mild preference for negative values corresponding to a decaying vacuum and energy transfer from dark energy to dark matter. Nevertheless, in both cases the coupling remains consistent with zero within  $2\sigma$ , and no statistically significant evidence for a dark sector interaction is found.

Among the models considered, the interacting vacuum model with  $Q \propto \rho_{\text{de}}$  gives the lowest  $\chi_{\text{min}}^2$ , improving the fit relative to  $\Lambda$ CDM by  $\Delta\chi^2 = -6.3$ . According to the Akaike Information

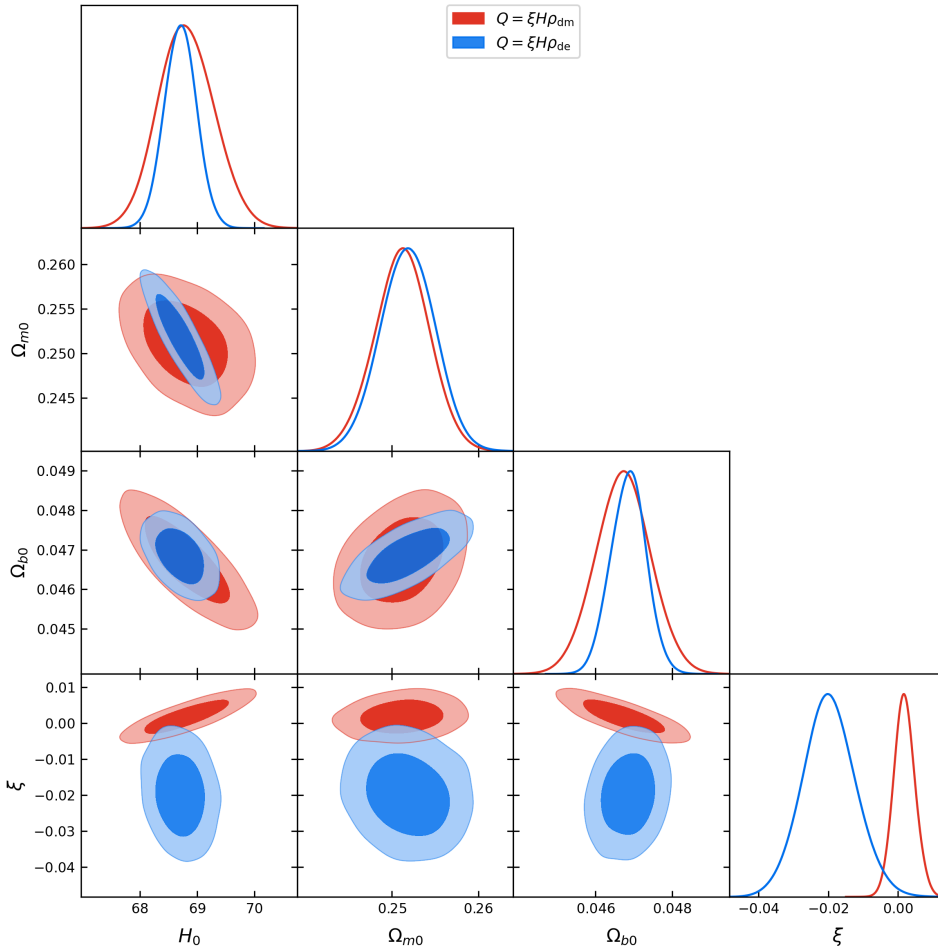


Figure 2: Marginalized one and two-dimensional posterior distributions for  $H_0$ ,  $\Omega_{m0}$ ,  $\Omega_{b0}$ , and the interaction parameter  $\xi$  obtained using background datasets ( $H(z)$ , Pantheon+ SNe, BAO, and CMB distance priors). The contours represent the 68% and 95% confidence regions for the two interaction prescriptions,  $Q = \xi H \rho_{\text{dm}}$  and  $Q = \xi H \rho_{\text{de}}$ , used to represent the diffusion model at the background level.

Criterion (AIC), this corresponds to  $\Delta\text{AIC} = -4.3$ , indicating a moderate statistical preference for this model despite the additional parameter. In contrast, the  $Q \propto \rho_{\text{dm}}$  model and the  $w\text{CDM}$  extension provide fits comparable to  $\Lambda\text{CDM}$  but are mildly disfavored once parameter complexity is taken into account. While the statistical improvement for the vacuum transfer case is non-negligible, it remains modest and does not constitute decisive evidence against  $\Lambda\text{CDM}$ .

Taken together, these results show that unimodular diffusion, interacting vacuum models with  $Q = \xi H \rho_{\text{dm}}$  or  $Q = \xi H \rho_{\text{de}}$ ,  $\Lambda\text{CDM}$ , and constant  $w$  dark energy models with  $w \simeq -1$  form a single equivalence class at the background level. Current background data constrain the expansion history of the Universe with high precision, but are intrinsically insensitive to the underlying microphysical origin of dark energy or dark sector interactions. Differences in the inferred values of the coupling parameter  $\xi$  reflect the model-dependent definition of the interaction term rather than physically distinct expansion dynamics.

## 7 Linear Perturbations and Growth of Structure

In the previous section we showed that unimodular diffusion, interacting vacuum models,  $\Lambda\text{CDM}$ , and  $w\text{CDM}$  form an equivalence class at the background level once the effective in-

Table 2: Mean values and  $1\sigma$  uncertainties for the model parameters in the interacting dark sector models,  $\Lambda$ CDM, and  $w$ CDM obtained from a joint analysis of  $H(z)$ , BAO DESI DR2, Pantheon+ SNIa, and CMB distance priors. The minimum  $\chi^2$  values and the corresponding differences  $\Delta\chi^2$  and  $\Delta\text{AIC}$  are quoted relative to  $\Lambda$ CDM.

Parameter	$Q = \xi H \rho_{\text{dm}}$	$Q = \xi H \rho_{\text{de}}$	$\Lambda$ CDM	$w$ CDM
$H_0$	$68.81 \pm 0.49$	$68.71 \pm 0.28$	$68.56 \pm 0.27$	$69.05 \pm 0.51$
$M_0$	$-19.367 \pm 0.015$	$-19.3700 \pm 0.0091$	$-19.3747 \pm 0.0087$	$-19.364 \pm 0.013$
$\alpha$	$0.1388 \pm 0.0042$	$0.1388 \pm 0.0043$	$0.1389 \pm 0.0043$	$0.1391 \pm 0.0042$
$\beta$	$2.510 \pm 0.073$	$2.514 \pm 0.074$	$2.513 \pm 0.072$	$2.519 \pm 0.074$
$\gamma$	$0.036 \pm 0.010$	$0.037 \pm 0.010$	$0.037 \pm 0.010$	$0.036 \pm 0.010$
$\Omega_{\text{dm}0}$	$0.2512 \pm 0.0032$	$0.2518 \pm 0.0031$	$0.2509 \pm 0.0031$	$0.2486 \pm 0.0038$
$\Omega_{b0}$	$0.04672 \pm 0.00072$	$0.04686 \pm 0.00046$	$0.04705 \pm 0.00046$	$0.04635 \pm 0.00077$
$\omega_{\text{de}}$ (fixed)	-1	-1	-1	$-1.025 \pm 0.021$
$\xi$	$0.0018 \pm 0.0031$	$-0.0197 \pm 0.0076$	0	0
$\chi_{\text{min}}^2$	1641.3	1634.5	1640.8	1641.7
$\Delta\chi^2$	0.5	-6.3	0	0.9
$\Delta\text{AIC}$	2.5	-4.3	0	2.9

interaction term is appropriately identified. Although current background observations tightly constrain the expansion history  $H(z)$ , they do not uniquely determine the microphysical origin of dark energy or dark sector interactions. To break this degeneracy, it is necessary to examine the evolution of cosmological perturbations. The growth of structure provides an independent and sensitive probe of energy exchange in the dark sector, since even small modifications to the conservation equations can alter the clustering dynamics of matter. In this section, we therefore analyze scalar perturbations and derive the corresponding growth equation, with particular emphasis on identifying the conditions under which unimodular diffusion remains perturbatively equivalent to phenomenological interacting vacuum models. We study scalar perturbations around a spatially flat Friedmann-Lemaître-Robertson-Walker (FLRW) background. In the Newtonian gauge the perturbed metric is

$$ds^2 = -(1 + 2\Psi)dt^2 + a^2(t)(1 - 2\Phi)\delta_{ij}dx^i dx^j. \quad (47)$$

The unimodular field equations can be rewritten in the Einstein form

$$G_{\mu\nu} = 8\pi G \left( T_{\mu\nu} + T_{\mu\nu}^{(\Lambda)} \right), \quad (48)$$

where the effective vacuum component is defined through an integration function  $P(t)$

$$\rho_{\Lambda}^{\text{eff}} = \frac{\Lambda}{8\pi G} + P(t). \quad (49)$$

The bare cosmological constant  $\Lambda$  is constant, while  $P(t)$  encodes the diffusion process. Energy-momentum conservation for the total matter plus vacuum is preserved, but the two components exchange energy according to

$$\dot{\rho}_c + 3H\rho_c = -\dot{P}, \quad \dot{\rho}_{\Lambda}^{\text{eff}} = \dot{P}, \quad (50)$$

Since our model preserves full diffeomorphism invariance ( $\delta\sqrt{-g} \neq 0$ ) and we consider the case diffusion function  $P(t)$  purely homogeneous and does not represent an independent dynamical field, its perturbation vanishes identically at linear order. Consequently,

$$\delta P(t) = \delta\dot{P}(t) = 0, \quad (51)$$

and the effective vacuum component remains spatially uniform. This is a key point, as a result the perturbed Einstein equations reduce to their standard general relativistic form. In particular the Poisson equation and the Euler equation for cold dark matter (CDM) read

$$\nabla^2\Phi = 4\pi G a^2 \rho_m \delta_m, \quad (52)$$

$$\dot{\theta}_c + H\theta_c = \frac{k^2}{a}\Phi, \quad (53)$$

where  $\delta_m = (\rho_c\delta_c + \rho_b\delta_b)/\rho_m$  is the total matter density contrast and  $\theta_c$  is the CDM velocity divergence. Baryons and radiation follow their usual equations and will be included in the full numerical solution, but for the derivation of the CDM growth equation they can be neglected in a first approximation.

The perturbed part of the conservation equation (50) for CDM, taking into account the diffusion is,

$$\dot{\delta}_c = -\frac{\theta_c}{a} + \frac{\dot{P}}{\rho_c}\delta_c - \frac{\delta\dot{P}}{\rho_c}, \quad (54)$$

As discussed above, in our formalism  $\delta\dot{P}(t) = 0$ , hence

$$\dot{\delta}_c = -\frac{\theta_c}{a} + \Gamma\delta_c, \quad \Gamma \equiv \frac{\dot{P}}{\rho_c}. \quad (55)$$

Taking a time derivative of (55) and using (53) to eliminate  $\dot{\theta}_c$  gives

$$\ddot{\delta}_c = -\frac{\dot{\theta}_c}{a} + \frac{H}{a}\theta_c + \dot{\Gamma}\delta_c + \Gamma\dot{\delta}_c = -\left(-\frac{H}{a}\theta_c + \frac{k^2}{a^2}\Phi\right) + \frac{H}{a}\theta_c + \dot{\Gamma}\delta_c + \Gamma\dot{\delta}_c. \quad (56)$$

The term  $\frac{\theta_c}{a}$  can be expressed from (55) as  $\frac{\theta_c}{a} = -\dot{\delta}_c + \Gamma\delta_c$ . Substituting and using the Poisson equation (52) to replace  $\Phi$ , we obtain

$$\ddot{\delta}_c + (2H - \Gamma)\dot{\delta}_c - \left[4\pi G\rho_m\delta_m + (2H\Gamma + \dot{\Gamma})\delta_c\right] = 0. \quad (57)$$

Equation (57) provides the exact linear evolution equation for the CDM density contrast in the presence of the unimodular diffusion function  $P(t)$ . Identifying  $\dot{P}(t) = Q(t)$ , the resulting growth equation coincides with that of interacting vacuum energy models with equation of state  $w = -1$  and interaction  $Q \propto \rho_\Lambda$ , provided the four-momentum transfer is purely timelike and  $\delta\rho_\Lambda = 0$  [63].

Importantly, Eq. (57) depends only on the background quantities  $H$ ,  $\rho_c$ ,  $\rho_\Lambda$ , and the effective interaction rate  $\Gamma \equiv Q/\rho_c$ , and is therefore insensitive to the microscopic origin of the energy exchange. Any theory yielding the same expansion history  $H(z)$  and interaction function  $\Gamma(z)$  predicts the same linear evolution of  $\delta_c(z)$ .

To connect with observations, we relate the growth equation to the observable  $f\sigma_8$ . Defining  $f \equiv d \ln \delta_c / d \ln a$  and using  $d/d \ln a = H^{-1}d/dt$ , Eq. (57) can be rewritten as

$$\frac{df}{d \ln a} + f^2 + \left(2 + \frac{\dot{H}}{H^2} - \frac{\Gamma}{H}\right) f = \frac{3}{2}\Omega_m + \frac{2\Gamma}{H} + \frac{\dot{\Gamma}}{H^2}, \quad (58)$$

Because Eqs. (58) coincide for unimodular diffusion and interacting vacuum energy models with homogeneous transfer at linear order, constraints derived from  $f\sigma_8$  measurements apply equally to both frameworks. Within this restricted subclass, growth data constrain only the effective transfer rate  $\Gamma(z)$  and do not distinguish between the geometric diffusion and its phenomenological interacting vacuum counterpart. Hence, under the assumptions of homogeneous  $P(t)$  and absence of momentum exchange, unimodular diffusion and interacting vacuum energy belong to the same dynamical equivalence class at the level of linear scalar perturbations.

Table 3: Compilation of redshift-space distortion (RSD) measurements of  $f\sigma_8(z)$  used in this work. The quoted uncertainties correspond to  $1\sigma$  errors. Data are taken from Ref. [64].

Dataset	$z$	$f\sigma_8(z)$
6dFGS+SnIa	0.02	$0.428 \pm 0.0465$
6dFGS	0.067	$0.423 \pm 0.055$
SDSS-MGS	0.15	$0.490 \pm 0.145$
2dFGRS	0.17	$0.510 \pm 0.060$
BOSS-LOWZ	0.32	$0.384 \pm 0.095$
SDSS-LRG-200	0.37	$0.4602 \pm 0.0378$
BOSS DR12	0.40	$0.473 \pm 0.086$
WiggleZ	0.44	$0.413 \pm 0.080$
SDSS-BOSS	0.50	$0.427 \pm 0.043$
BOSS CMASS	0.57	$0.426 \pm 0.029$
WiggleZ	0.60	$0.390 \pm 0.063$
WiggleZ	0.73	$0.437 \pm 0.072$
VVDS	0.77	$0.490 \pm 0.180$
Vipers	0.80	$0.470 \pm 0.080$
Vipers PDR-2	0.86	$0.400 \pm 0.110$
Vipers v7	1.05	$0.280 \pm 0.080$
FastSound	1.40	$0.482 \pm 0.116$
SDSS-IV	1.52	$0.396 \pm 0.079$
SDSS-IV	1.944	$0.364 \pm 0.106$

To constrain the modified growth equation with observations, we use redshift-space distortion (RSD) measurements of the quantity  $f\sigma_8(z)$ , which directly probe the linear growth rate of matter perturbations. We adopt a compilation of independent measurements spanning the redshift range  $z \leq 2$  from Ref. [64], summarized in Table 3. The RSD measurements used in this work are reported assuming a fiducial  $\Lambda$ CDM cosmology. Since the interacting models considered here produce expansion histories that do not deviate significantly from the fiducial model, the Alcock-Paczynski rescaling is expected to introduce only subdominant corrections compared to current observational uncertainties. For simplicity, we therefore neglect this effect in the present analysis. The RSD data are included in the joint likelihood in order to assess how growth measurements constrain the interaction parameter  $\xi$ .

The interaction considered here does not modify the gravitational sector and involves purely timelike energy transfer, with homogeneous vacuum perturbations ( $\delta P = 0$ ). Under these assumptions, the linear growth equation for cold dark matter remains scale-independent on subhorizon scales. So, the matter power spectrum can be written as [65],

$$P_m(k, z) = D^2(z)P_m(k, 0), \quad (59)$$

where growth factor  $D(z)$  is obtained from the definition  $f = d \ln D / d \ln a$ , which gives

$$D(a) = \exp\left(\int_{a_i}^a f(a') d \ln a'\right). \quad (60)$$

The normalization is chosen such that  $D(a = 1) = 1$ . The present-day clustering amplitude is parameterized through

$$S_8 = \sigma_{8,0} \sqrt{\frac{\Omega_{m0}}{0.3}}, \quad (61)$$

with  $S_8$  treated as a free parameter. The observable quantities are therefore computed as

$$\sigma_8(z) = \sigma_{8,0}D(z), \quad f\sigma_8(z) = f(z)\sigma_{8,0}D(z), \quad (62)$$

where  $\sigma_{8,0} = S_8/\sqrt{\Omega_{m0}/0.3}$ . The background evolution is constrained using CMB distance priors, while the redshift dependence of clustering follows directly from the scale-independent growth factor.

The impact of including growth measurements on the parameter  $\xi$  is illustrated in Fig. 3. For the diffusion model, background-only data yield  $\xi = -0.0197 \pm 0.0076$ , corresponding to a

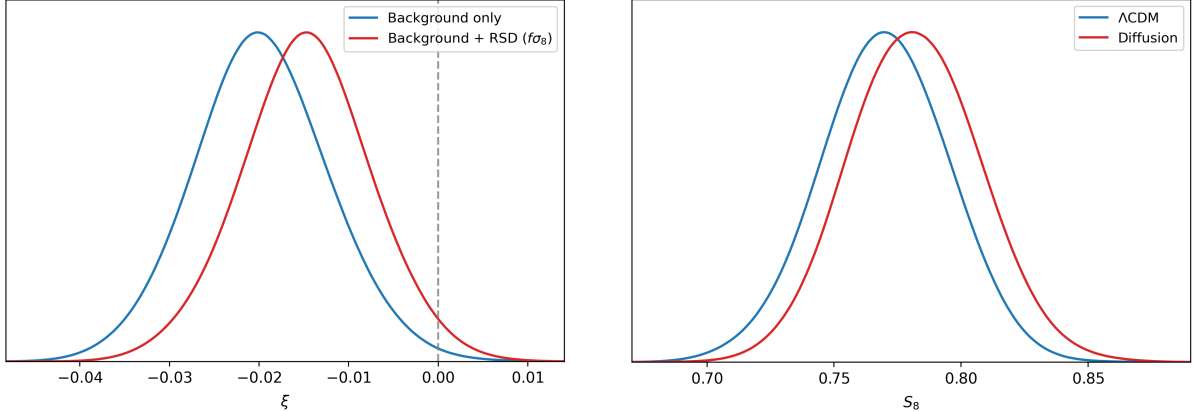


Figure 3: Left: One dimensional posterior distributions of the interaction parameter  $\xi$  for the diffusion model  $Q = \xi H \rho_\Lambda$  using background-only data and the combined background+RSD analysis. Right: Corresponding constraints on  $S_8$  for  $\Lambda$ CDM and the diffusion model using the full dataset. Growth measurements mildly reduce the statistical preference for nonzero  $\xi$  while inducing only a modest shift in  $S_8$ .

$\sim 2.6\sigma$  indication of a small negative coupling. When  $f\sigma_8$  measurements are included, the constraint shifts to  $\xi = -0.0146 \pm 0.0075$ , reducing the statistical significance to approximately  $2\sigma$ . Correspondingly, the improvement in goodness-of-fit relative to  $\Lambda$ CDM seen in the background-only analysis ( $\Delta\chi^2 = -6.3$ ) is removed once growth data are included, yielding  $\Delta\chi^2 = +1.37$  for the full dataset. Thus, the preference for interaction present in the background-only analysis is not maintained once large-scale structure measurements are taken into account.

For the combined dataset considered here,  $\Lambda$ CDM gives  $S_8 = 0.77 \pm 0.025$ , which is lower than the Planck  $\Lambda$ CDM value  $S_8 \approx 0.83$ . The diffusion model shifts this value slightly upward to  $S_8 = 0.782 \pm 0.026$ , although it remains below the Planck result. This difference mainly reflects the absence of the full CMB power spectrum likelihood in our analysis, rather than a strong model-dependent effect.

The corresponding predictions for the growth observable  $f\sigma_8(z)$  are shown in Fig. 4, where both the diffusion model and the  $\Lambda$ CDM model provide nearly identical growth histories within the current observational uncertainties. The diffusion model produces a slightly higher clustering amplitude, consistent with the modest upward shift in  $S_8$ , but the difference remains well within the error bars of the present redshift-space distortion measurements. Taken together, these results indicate that although the perturbation analysis restricts the background equivalence class to homogeneous interacting vacuum models, current growth data do not provide statistically significant evidence for a nonzero interaction. Consequently, the diffusion model remains observationally consistent with  $\Lambda$ CDM, and the degeneracy between the two descriptions is only weakly lifted by present large-scale structure measurements.

It is important to emphasize that the perturbative equivalence established above does not extend to arbitrary interacting dark sector models, but only to a restricted subclass. In this work we adopt the fully diffeomorphism-invariant formulation of unimodular gravity, for which  $\delta\sqrt{-g} \neq 0$ . In this formulation the gravitational sector and gauge structure coincide with those of general relativity, allowing the use of standard Newtonian or synchronous gauge perturbation theory. Constrained unimodular formulations with  $\delta\sqrt{-g} = 0$  possess reduced gauge freedom

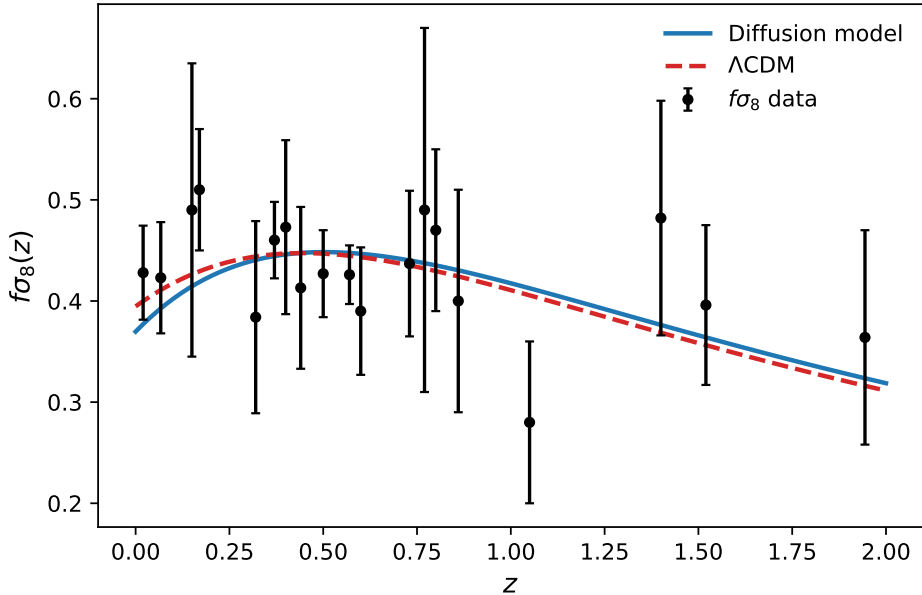


Figure 4: Evolution of the growth-rate observable  $f\sigma_8(z)$ . The blue solid curve shows the best-fit prediction of the diffusion model, while the red dashed curve corresponds to the  $\Lambda$ CDM prediction obtained using the same dataset combination. Black points with error bars represent redshift-space distortion (RSD) measurements of  $f\sigma_8$ . The two models produce nearly identical growth histories within current observational uncertainties, indicating that present large-scale structure data do not strongly distinguish between diffusion-driven vacuum dynamics and the standard  $\Lambda$ CDM model.

and lead to modified perturbation equations, which lie beyond the scope of the present analysis.

In the unimodular diffusion framework the integration function  $P(t)$  is purely homogeneous by construction. Consequently  $\delta P = 0$  and, since  $Q = \dot{P}$ , one also has  $\delta Q = 0$ . The perturbed CDM continuity equation therefore depends only on the background interaction rate  $\Gamma = Q/\rho_c$  and contains no intrinsic perturbation of the transfer term.

In phenomenological interacting dark energy models, however, the perturbation  $\delta Q$  depends explicitly on the chosen coupling prescription. For example, if  $Q \propto \rho_c$  one typically obtains

$$\delta Q \propto \delta \rho_c, \quad (63)$$

which directly modifies the matter growth equation at linear order. This statement assumes the commonly adopted choice of vanishing momentum transfer in the dark matter rest frame,  $Q^\mu = Qu_{\text{dm}}^\mu$ , such that the energy exchange is purely timelike and aligned with the dark matter four-velocity.

By contrast, for interacting vacuum models with  $Q \propto \rho_\Lambda$ ,  $w = -1$ , and vanishing vacuum perturbations  $\delta \rho_\Lambda = 0$ , the perturbed transfer term becomes

$$\delta Q = \xi \rho_\Lambda \delta H. \quad (64)$$

On subhorizon scales metric perturbations are suppressed relative to matter density fluctuations, leaving  $\delta H$  and therefore  $\delta Q$  subdominant. In this regime the resulting growth equation coincides with that obtained in the unimodular diffusion framework.

Therefore the perturbative equivalence with unimodular diffusion holds only for interacting vacuum energy models in which the transfer term remains effectively homogeneous at linear order in the subhorizon limit. More general interacting models, where  $\delta Q$  inherits clustering from  $\delta \rho_c$  or additional metric perturbations, lead to distinguishable signatures in the growth rate

and large-scale structure observables, providing a potential observational test of the diffusion framework. Relaxing any of these assumptions would modify the perturbation equations and break the degeneracy between unimodular diffusion and interacting vacuum energy. Within the framework considered here, however, these conditions are satisfied by construction.

## 8 Conclusion

In this work we clarified the correspondence between unimodular diffusion cosmology and interacting dark sector models. By identifying the diffusion rate with an effective energy transfer term,  $Q = -\dot{P}$ , we showed that unimodular diffusion maps onto interacting vacuum models with  $w_{\text{de}} = -1$  at the background level. This mapping implies that the diffusion framework does not generate a distinct expansion history but instead provides a geometric realization of the interacting vacuum class. At the background level, both the vacuum-coupled ( $Q = \xi H \rho_{\text{de}}$ ) and matter-coupled ( $Q = \xi H \rho_{\text{dm}}$ ) parameterizations fit the data comparably. However, at linear perturbation level only the vacuum-coupled interaction remains consistent with the diffusion framework.

Using cosmic chronometer  $H(z)$  data, Pantheon+ supernovae, DESI BAO, and CMB distance priors, we obtained  $\xi = -0.0197 \pm 0.0076$  for the vacuum-coupled case. Including redshift-space distortion measurements ( $f\sigma_8$ ) shifts the constraint to  $\xi = -0.0147 \pm 0.0075$ , which remains consistent with  $\Lambda$ CDM ( $\xi = 0$ ) at the  $2\sigma$  level. The corresponding clustering amplitudes,  $S_8 = 0.77 \pm 0.025$  for  $\Lambda$ CDM and  $S_8 = 0.782 \pm 0.026$  for the diffusion model (with the same datasets), indicate a modest impact on late-time structure growth.

At the perturbative level, the defining condition of the unimodular diffusion framework is  $\delta P = 0$  (equivalently  $\delta Q = 0$ ), which reflects the homogeneity of the diffusion function and the absence of momentum transfer. Under this condition, together with full diffeomorphism invariance, purely timelike energy transfer, and the sub-horizon linear regime, the CDM growth equation in unimodular diffusion coincides exactly with that of interacting vacuum models sharing the same  $Q(t)$ . Consequently, linear observables,  $f$ ,  $D(z)$ , and  $f\sigma_8(z)$ , depend only on the effective transfer rate  $\Gamma = Q/\rho_c$  and the background expansion  $H(z)$ , making them insensitive to the microscopic origin of the interaction. Within the linear regime, unimodular diffusion and homogeneous interacting vacuum models thus belong to the same dynamical equivalence class. The matter-coupled interaction, on the other hand, does not satisfy  $\delta Q = 0$  and therefore does not represent a perturbatively consistent class of the diffusion model.

Our results indicate that current cosmological observations based on the homogeneous expansion history and linear perturbations constrain only the effective energy exchange in the dark sector. They do not differentiate between its geometric realization in unimodular diffusion and its phenomenological description in interacting vacuum models. Although linear perturbations restrict the background equivalence class to homogeneous vacuum transfer models, present growth measurements do not break the degeneracy with  $\Lambda$ CDM.

Future efforts to differentiate these frameworks will likely require probes sensitive to momentum transfer, non-linear structure formation, or deviations from standard gravitational dynamics beyond the linear regime. Hence, unimodular diffusion stands as a consistent and perturbatively stable extension of standard cosmology that remains compatible with current data while highlighting the theoretical degeneracies inherent in linear cosmological observations.

## Acknowledgements

GK acknowledges Vellore Institute of Technology for the financial support through its Seed Grant (No.SG20230035), year 2023.

## References

- [1] PLANCK collaboration, *Planck 2018 results. VI. Cosmological parameters*, *Astron. Astrophys.* **641** (2020) A6 [1807.06209].
- [2] A.G. Riess, S. Casertano, W. Yuan, J.B. Bowers, L. Macri, J.C. Zinn et al., *Cosmic Distances Calibrated to 1% Precision with Gaia EDR3 Parallaxes and Hubble Space Telescope Photometry of 75 Milky Way Cepheids Confirm Tension with  $\Lambda$ CDM*, *Astrophys. J. Lett.* **908** (2021) L6 [2012.08534].
- [3] H0LiCOW collaboration, *H0LiCOW - IX. Cosmographic analysis of the doubly imaged quasar SDSS 1206+4332 and a new measurement of the Hubble constant*, *Mon. Not. Roy. Astron. Soc.* **484** (2019) 4726 [1809.01274].
- [4] DESI collaboration, *DESI 2024 VI: cosmological constraints from the measurements of baryon acoustic oscillations*, *JCAP* **02** (2025) 021 [2404.03002].
- [5] DESI collaboration, *DESI DR2 Results II: Measurements of Baryon Acoustic Oscillations and Cosmological Constraints*, 2503.14738.
- [6] T.P. Sotiriou and V. Faraoni,  *$f(R)$  Theories Of Gravity*, *Rev. Mod. Phys.* **82** (2010) 451 [0805.1726].
- [7] A.A. Starobinsky, *Disappearing cosmological constant in  $f(R)$  gravity*, *JETP Lett.* **86** (2007) 157 [0706.2041].
- [8] S. Nojiri and S.D. Odintsov, *Modified  $f(R)$  gravity consistent with realistic cosmology: From matter dominated epoch to dark energy universe*, *Phys. Rev. D* **74** (2006) 086005 [hep-th/0608008].
- [9] S. Nojiri and S.D. Odintsov, *Unified cosmic history in modified gravity: From  $f(r)$  theory to lorentz non-invariant models*, *Physics Reports* **505** (2011) 59.
- [10] S. Nojiri, S. Odintsov and V. Oikonomou, *Modified gravity theories on a nutshell: Inflation, bounce and late-time evolution*, *Physics Reports* **692** (2017) 1.
- [11] T. Chiba,  *$W$  and  $w'$  of scalar field models of dark energy*, *Phys. Rev. D* **73** (2006) 063501 [astro-ph/0510598].
- [12] S. Tsujikawa, *General analytic formulae for attractor solutions of scalar-field dark energy models and their multi-field generalizations*, *Phys. Rev. D* **73** (2006) 103504 [hep-th/0601178].
- [13] S. Tsujikawa, *Reconstruction of general scalar-field dark energy models*, *Phys. Rev. D* **72** (2005) 083512 [astro-ph/0508542].
- [14] E.J. Copeland, M. Sami and S. Tsujikawa, *Dynamics of dark energy*, *Int. J. Mod. Phys. D* **15** (2006) 1753 [hep-th/0603057].
- [15] S.N. K. Bamba, S. Capozziello and S.D. Odintsov, *Dark energy cosmology: the equivalent description via different theoretical models and cosmography tests*, *Astrophys. Space Sci* **342** (2012) 155.
- [16] R.-Y. Guo, L. Feng, T.-Y. Yao and X.-Y. Chen, *Exploration of interacting dynamical dark energy model with interaction term including the equation-of-state parameter: alleviation of the  $H_0$  tension*, *JCAP* **12** (2021) 036 [2110.02536].

- [17] R. Murgia, S. Gariazzo and N. Fornengo, *Constraints on the Coupling between Dark Energy and Dark Matter from CMB data*, *JCAP* **04** (2016) 014 [1602.01765].
- [18] B. Hu and Y. Ling, *Interacting dark energy, holographic principle and coincidence problem*, *Phys. Rev. D* **73** (2006) 123510 [hep-th/0601093].
- [19] H.M. Sadjadi and M. Alimohammadi, *Cosmological coincidence problem in interactive dark energy models*, *Phys. Rev. D* **74** (2006) 103007 [gr-qc/0610080].
- [20] M.S. Berger and H. Shojaei, *Interacting dark energy and the cosmic coincidence problem*, *Phys. Rev. D* **73** (2006) 083528 [gr-qc/0601086].
- [21] T.-N. Li, P.-J. Wu, G.-H. Du, S.-J. Jin, H.-L. Li, J.-F. Zhang et al., *Constraints on Interacting Dark Energy Models from the DESI Baryon Acoustic Oscillation and DES Supernovae Data*, *Astrophys. J.* **976** (2024) 1 [2407.14934].
- [22] S. Pan, S. Paul, E.N. Saridakis and W. Yang, *Interacting dark energy after DESI DR2: a challenge for  $\Lambda$ CDM paradigm?*, 2504.00994.
- [23] E. Silva, M.A. Sabogal, M.S. Souza, R.C. Nunes, E. Di Valentino and S. Kumar, *New Constraints on Interacting Dark Energy from DESI DR2 BAO Observations*, 2503.23225.
- [24] K.L. Pandey, T. Karwal and S. Das, *Alleviating the  $H_0$  and  $\sigma_8$  anomalies with a decaying dark matter model*, *JCAP* **07** (2020) 026 [1902.10636].
- [25] C. Corral, N. Cruz and E. González, *Diffusion in unimodular gravity: Analytical solutions, late-time acceleration, and cosmological constraints*, *Phys. Rev. D* **102** (2020) 023508.
- [26] F.X. Linares Cedeño and U. Nucamendi, *Revisiting cosmological diffusion models in unimodular gravity and the  $h_0$  tension*, *Physics of the Dark Universe* **32** (2021) 100807.
- [27] S.J. Landau, M. Benetti, A. Perez and D. Sudarsky, *Cosmological constraints on unimodular gravity models with diffusion*, *Phys. Rev. D* **108** (2023) 043524.
- [28] T. Josset, A. Perez and D. Sudarsky, *Dark energy from violation of energy conservation*, *Phys. Rev. Lett.* **118** (2017) 021102.
- [29] B. Kursunoglu, S.L. Mintz and A. Perlmutter, eds., *HIGH-ENERGY PHYSICS. PROCEEDINGS, 20TH ANNUAL ORBIS SCIENTIAE, MIAMI, USA, JANUARY 17-21, 1983*, 1985.
- [30] W. Buchmüller and N. Dragon, *Einstein gravity from restricted coordinate invariance*, *Physics Letters B* **207** (1988) 292.
- [31] W.G. Unruh, *Unimodular theory of canonical quantum gravity*, *Phys. Rev. D* **40** (1989) 1048.
- [32] P. Jain, P. Karmakar, S. Mitra, S. Panda and N.K. Singh, *Testing unimodular gravity*, *Journal of Cosmology and Astroparticle Physics* **2012** (2012) 020.
- [33] P. Jain, A. Jaiswal, P. Karmakar, G. Kashyap and N.K. Singh, *Cosmological implications of unimodular gravity*, *Journal of Cosmology and Astroparticle Physics* **2012** (2012) 003.
- [34] E. Álvarez, *Can one tell einstein's unimodular theory from einstein's general relativity?*, *Journal of High Energy Physics* **2005** (2005) 002.
- [35] E. Álvarez and A.F. Faedo, *Unimodular cosmology and the weight of energy*, *Phys. Rev. D* **76** (2007) 064013.

- [36] C. Gao, R. Brandenberger, Y. Cai and P. Chen, *Cosmological perturbations in unimodular gravity*, *Journal of Cosmology and Astroparticle Physics* **2014** (2014) .
- [37] S. Nojiri, S.D. Odintsov and V.K. Oikonomou, *Unimodular-mimetic cosmology*, *Classical and Quantum Gravity* **33** (2016) 125017.
- [38] K. Bamba, S.D. Odintsov and E.N. Saridakis, *Inflationary cosmology in unimodular  $f(t)$  gravity*, *Modern Physics Letters A* **32** (2017) 1750114.
- [39] F. Rajabi and K. Nozari, *Unimodular  $f(r,t)$  gravity*, *Physical Review D* **96** (2017) .
- [40] F. Rajabi and K. Nozari, *Energy condition in unimodular  $f(r, t)$  gravity*, *European Physical Journal C* **81** (2021) .
- [41] A. Costantini and E. Elizalde, *A reconstruction method for anisotropic universes in unimodular  $F(R)$ -gravity*, *Eur. Phys. J. C* **82** (2022) 1127 [2212.02568].
- [42] I. Cho and N.K. Singh, *Unimodular theory of gravity and inflation*, *Classical and Quantum Gravity* **32** (2015) 135020.
- [43] N.K. SINGH, *Unimodular constraint on global scale invariance*, *Modern Physics Letters A* **28** (2013) 1350130 [<https://doi.org/10.1142/S0217732313501307>].
- [44] S.D. Odintsov and V.K. Oikonomou, *Unimodular mimetic  $F(R)$  inflation*, *Astrophysics and Space Science* **361** (2016) 236 [1602.05645].
- [45] F. Linares Cedeño and U. Nucamendi, *Revisiting cosmological diffusion models in unimodular gravity and the  $h_0$  tension*, *Physics of the Dark Universe* **32** (2021) .
- [46] A. Agrawal, B. Mishra and P. Moraes, *Unimodular gravity traversable wormholes*, *European Physical Journal Plus* **138** (2023) .
- [47] N.K. Singh and G. Kashyap, *Unimodular theory of gravity in light of the latest cosmological data*, *Universe* **9** (2023) .
- [48] R. Jimenez and A. Loeb, *Constraining cosmological parameters based on relative galaxy ages*, *The Astrophysical Journal* **573** (2002) 37.
- [49] D. Scolnic, D. Brout, A. Carr, A.G. Riess, T.M. Davis, A. Dwomoh et al., *The pantheon+ analysis: The full data set and light-curve release*, *The Astrophysical Journal* **938** (2022) 113.
- [50] DESI COLLABORATION collaboration, *Desi dr2 results. ii. measurements of baryon acoustic oscillations and cosmological constraints*, *Phys. Rev. D* **112** (2025) 083515.
- [51] L. Chen, Q.-G. Huang and K. Wang, *Distance priors from planck final release*, *Journal of Cosmology and Astroparticle Physics* **2019** (2019) 028.
- [52] C. Zhang, H. Zhang, S. Yuan, S. Liu, T.-J. Zhang and Y.-C. Sun, *Four new observational  $H(z)$  data from luminous red galaxies in the Sloan Digital Sky Survey data release seven*, *Research in Astronomy and Astrophysics* **14** (2014) 1221 [1207.4541].
- [53] M. Moresco, L. Pozzetti, A. Cimatti, R. Jimenez, C. Maraston, L. Verde et al., *A 6% measurement of the Hubble parameter at  $z \sim 0.45$ : direct evidence of the epoch of cosmic re-acceleration*, *Journal of Cosmology and Astroparticle Physics* **05** (2016) 014 [1601.01701].

- [54] R. Jimenez, L. Verde, T. Treu and D. Stern, *Constraints on the equation of state of dark energy and the Hubble constant from stellar ages and the CMB*, *Astrophys. J.* **593** (2003) 622 [astro-ph/0302560].
- [55] D. Stern, R. Jimenez, L. Verde, M. Kamionkowski and S.A. Stanford, *Cosmic chronometers: constraining the equation of state of dark energy. i:  $H(z)$  measurements*, *Journal of Cosmology and Astroparticle Physics* **2010** (2010) 008.
- [56] M. Moresco, A. Cimatti, R. Jimenez, L. Pozzetti, G. Zamorani, M. Bolzonella et al., *Improved constraints on the expansion rate of the Universe up to  $z \approx 1.1$  from the spectroscopic evolution of cosmic chronometers*, *Journal of Cosmology and Astroparticle Physics* **2012** (2012) 006 [1201.3609].
- [57] J. Simon, L. Verde and R. Jimenez, *Constraints on the redshift dependence of the dark energy potential*, *Phys. Rev. D* **71** (2005) 123001 [astro-ph/0412269].
- [58] N. Borghi, M. Moresco and A. Cimatti, *Toward a better understanding of cosmic chronometers: A new measurement of  $h(z)$  at  $z = 0.7$* , *The Astrophysical Journal Letters* **928** (2022) L4.
- [59] M. Moresco, *Raising the bar: new constraints on the Hubble parameter with cosmic chronometers at  $z \sim 2$ .*, *Monthly Notices of the Royal Astronomical Society* **450** (2015) L16 [1503.01116].
- [60] A.L. Ratsimbazafy, S.I. Loubser, S.M. Crawford, C.M. Cress, B.A. Bassett, R.C. Nichol et al., *Age-dating Luminous Red Galaxies observed with the Southern African Large Telescope*, *Mon. Not. Roy. Astron. Soc.* **467** (2017) 3239 [1702.00418].
- [61] A. Verma, P.K. Aluri and D.F. Mota, *Anisotropic universe with anisotropic dark energy*, *Phys. Rev. D* **111** (2025) 083508.
- [62] D. Foreman-Mackey, D.W. Hogg, D. Lang and J. Goodman, *emcee: The mcmc hammer*, *Publications of the Astronomical Society of the Pacific* **125** (2013) 306.
- [63] T. Clemson, K. Koyama, G.-B. Zhao, R. Maartens and J. Väliviita, *Interacting dark energy: Constraints and degeneracies*, *Phys. Rev. D* **85** (2012) 043007.
- [64] L. Kazantzidis and L. Perivolaropoulos, *Evolution of the  $f\sigma_8$  tension with the Planck15/ $\Lambda$ CDM determination and implications for modified gravity theories*, *Phys. Rev. D* **97** (2018) 103503.
- [65] S. Dodelson, *Modern Cosmology*, Elsevier Science Publishing Co Inc (2003).